RSC Advances

ROYAL SOCIETY OF CHEMISTRY

www.rsc.org/advances

RSC Advances

ARTICLE

# A CO₂ Fixation Process with Waste Cement Powder via Regeneration of Alkali and Acid by Electrodialysis

Daiki Shuto,[a] Hiroki Nagasawa,[b] Atsushi Iizuka[c] and Akihiro Yamasaki[a]

A mineral carbonation process for CO_2 sequestration has been developed, and its process feasibility was examined based on laboratory-scale experimental studies. The process is composed of four steps: (i) Extraction of calcium ions from waste cement powder with nitric acid. (ii) Absorption of CO_2 in sodium hydroxide solution from CO_2 emission sources. (iii) Precipitation of calcium carbonate particles by mixing the calcium leached solution and the CO_2 absorbed solution. (iv) Regeneration of nitric acid and sodium hydroxide from the remaining solution of sodium nitrate from step (iii) with bipolar membrane electrodialysis. The regenerated acid and alkali can be reused in steps (i) and (ii) with newly fed waste cement powder. The overall mass balance of the process is the input of CO_2 and calcium and the output of calcium carbonate and residues of the leaching. The effects of the operation conditions in the calcium leaching step (i) and regeneration step (iv) were experimentally investigated with a laboratory-scale experimental apparatus. It was found that calcium leaching can be easily and quickly performed with nitric acid, and high-purity calcium carbonate can be obtained when the operation conditions are set to obtain a final pH of about 7. Regeneration of nitric acid and sodium hydroxide were favourable when the current density and the electric potential were high and the feed concentration was low in terms of the power consumption. Thus, the total process can be operated under appropriate conditions, and its CO_2 fixation performance was evaluated.

Introduction

Carbon capture and storage (CCS) has been recognized as an effective countermeasure for global warming [1, 2]. The main target of CCS is CO_2 generated in large-scale stationary sources such as thermal power plants, the cement industry, and the steel-making industry. The CO_2 in flue gas from these sources can be captured and stored in proper locations rather than being released into the atmosphere [3]. CCS technologies can be categorized into three types depending on the storage forms: geological, ocean, and mineral carbonation.[1] In this study, we focused on the mineral carbonation process, which is similar to the naturally occurring rock weathering reaction expressed; for example, by the following equations [4-6]:

$$CaSiO_3 + CO_2 \rightarrow CaCO_3 + SiO_2 \qquad (1)$$
$$MgSiO_3 + CO_2 \rightarrow MgCO_3 + SiO_2 \qquad (2)$$
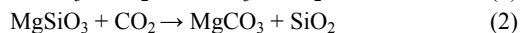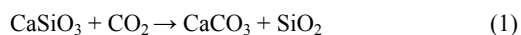
CO_2 is to be fixed as carbonates, which have large negative Gibbs energies of formation, indicating thermodynamically stable structures. The safety and stability of the products is the main advantage of the mineral carbonation process over other options. The mineral carbonation process, however, requires a huge amount of the fixation media containing alkali earth metals to match the CO_2 to be

fixed. Ultramafic rocks containing calcium or magnesium, such as wollastonite ($CaSiO_3$), olivine (Mg_2SiO_4), and serpentine ($Mg_3Si_2O_5(OH)_4$),[7-9] are rich in alkali earth metals and the carbonation reactions of these ultramafic rocks have been intensively studied. In addition, industrial wastes containing calcium, such as waste concrete, concrete sludge, steel slug, red mud, and fly ash, have been tested as CO_2 fixation media.[10-15] The reaction rates for the carbonation reaction with these resources are rather slow, and it has been recognized that acceleration of the reaction is important for practical implementation of the process. One possible way to accelerate the reaction is the use of acids for leaching calcium or magnesium from the source materials.[4-6, 15-21] Direct contact between the leached solution and flue gas or pure CO_2 gas forms carbonates as a precipitant. However, when a strong acid is used for leaching, the precipitation process requires high-pressure conditions of CO_2 to form calcium carbonate, increasing both the power consumption and the cost of the fixation process. The carbonate precipitation reaction would occur more easily by mixing the leached solution with alkaline carbonate solution, which is formed by the chemical absorption process of CO_2 from the flue gas with an alkaline solution. Teir *et al.* estimated that about 2.4 tons of sodium hydroxide and 2 to 4 tons of acid would be required to fix 1 ton of CO_2 in this process.[18]

The production of these products is also power consuming, and a life cycle analysis (LCA) demonstrated that net CO_2 fixation could be negative when this acid and alkali are used without regeneration.[19]

The acids used in the leaching processes, therefore, should be recycled and reused to make the process a practical option for CO_2 fixation. Regeneration of the acid should be accompanied by the regeneration of the alkali that was used for the chemical absorption process. The challenge is to develop an energy-efficient regeneration process of the acid and alkali from the solution after carbonate precipitation.

In this study, we examined the applicability of the electrodialysis method for the recovery of acid and alkali using a bipolar membrane (BMED).[22, 23] The bipolar membrane is a composite membrane composed of a cation exchange membrane and an anion exchange membrane. When an electric potential higher than the water dissociation potential (0.83 V) is applied across the membrane, the water contained in the membrane will be electrically dissociated, protons will be released through the cation exchange membrane, and hydroxide ions will be released through the anion exchange membrane. Figure 1 shows the schematic drawing of the BMED cells for nitric acid-sodium hydroxide recovery from sodium nitrate. The alkali recovery cell is formed by a bipolar membrane (BPM1) and a cation exchange membrane (CEM), and the acid recovery cell is formed by the cation exchange membrane and another bipolar membrane (BPM2). Sodium nitrate solution is introduced as feed both cells. Sodium ions in the feed solution introduced into the acid recovery cell will be transported to the alkali recovery cell through the cation exchange membrane driven by the electric potential. The sodium ions transported to the alkali recovery cell will be coupled with hydroxide ions generated from the bipolar membrane (BPM1) composing the alkali recovery cell. The nitrate ions will remain in the acid recovery cell, and couple with protons generated from the bipolar membrane (BPM 2) to form nitric acid. Thus, nitric acid and sodium hydroxide can be recovered by the BMED method. The main advantage of the BMED is that no additional chemicals are required for the regeneration: only the membranes and electric power are required. The efficiency of the BMED step could be significantly improved by process design through the optimization of various operation parameters.
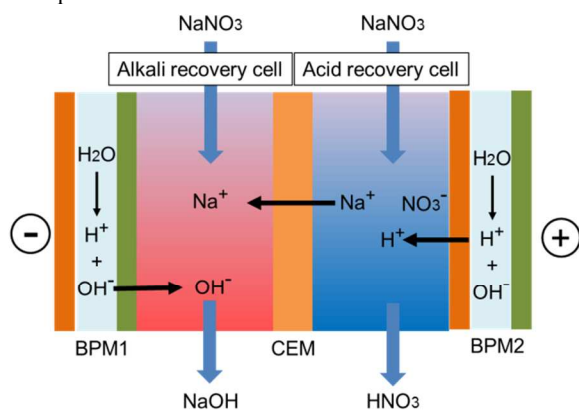

Fig. 1 Schematic drawing for the acid and alkali recovery mechanism with BMED. BPM1, BPM2; bipolar membranes, CEM; cation exchange membrane. Bipolar membrane is a composite membrane of laminated CEM and AEM (anion exchange membrane). When an electric potential higher than the dissociation potential of the water molecule (0.83 V) is applied, the water in the membrane dissociates to a proton and a hydroxide ion. The proton is released

from the CM side and the hydroxide ion is released from the AM side.

We proposed in this study a new type of CO_2 fixation process by utilizing the BMED process. A schematic flow diagram of the proposed process is shown in Figure 2. The process is composed of four steps:

(i) Extraction of calcium: an acid solution such as nitric acid is used for the extraction of calcium ions from calcium or magnesium sources.

$$\text{(Ca or Mg)} \xrightarrow{2H^+} Ca^{2+} \text{ (or } Mg^{2+}) \qquad (3)$$
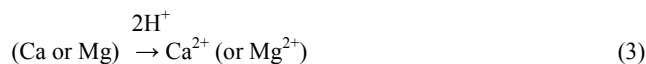
(ii) CO_2 absorption: CO_2 is captured from flue gas into an alkaline hydroxide solution, such as sodium or potassium hydroxide, to form sodium carbonate solution.

$$2Na^+ \text{ (or } 2K^+) + 2OH^- + CO_2(g) \\ \rightarrow 2Na^+ \text{(or } 2K^+) + CO_3^{2-} + H_2O \qquad (4)$$
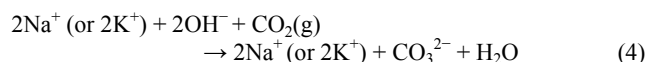
(iii) Precipitation of carbonate: calcium or magnesium carbonate is crystallized and precipitated by mixing the solutions from steps (i) and (ii).

$$Ca^{2+} \text{ (or } Mg^{2+}) + CO_3^{2-} \rightarrow CaCO_3 \text{ (or } MgCO_3) \qquad (5)$$
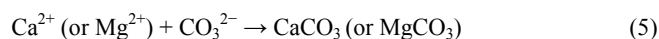
(iv) Regeneration of acid and alkali by BMED: the neutralized solution is treated in the BMED to regenerate the acid and the alkali, which can then be reused for steps (i) and (ii).

$$Na^+ \text{(or } K^+) + NO_3^- + H_2O \rightarrow \{Na^+ \text{(or } K^+)+OH^-\}+ \{H^+ + NO_3^-\} \quad (6)$$
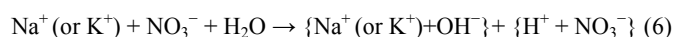
The complete reaction is shown within the process boundary indicated by the dotted line in Figure 2. The inputs are CO_2 and magnesium and/or calcium, and the output is the corresponding carbonate. Some residues would also be formed depending on the calcium or magnesium sources. The overall process does not require the addition of acid and alkali when the process perfectly proceeds.
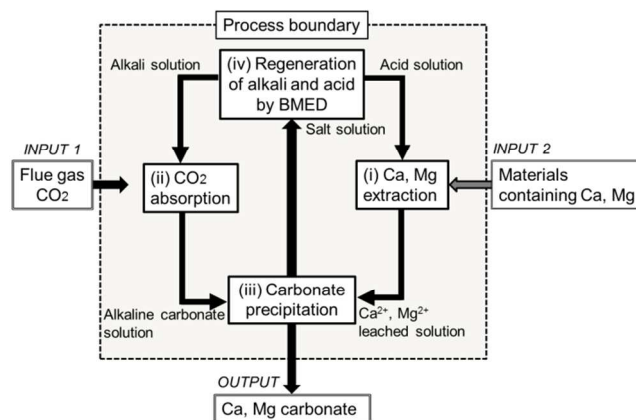
Fig. 2 Flow diagram of the CO_2 fixation process.

Waste cement powder was used as an alkali earth metal (calcium) source in this study. The waste cement powder is a byproduct of the recycling process of aggregates from waste cement generated from

demolished concrete buildings. The waste concrete generation rate is about 30 million metric tons annually in Japan.[24] Annual generation in the EU is as large as 330 million metric tons (2007).[25] In the United States, the generation of waste concrete is estimated to be several tens of million metric tons per year.[26] In China, the generation of waste concrete is rapidly increasing because of the rapid cycle of construction and demolition of concrete buildings, and it has been estimated that the amount of waste concrete produced in China will be 1.5 billion metric tons in 2030 and 5.4 billion metric tons in 2050.[27] In Japan, recycling processes of aggregates from waste concrete have been developed. In the recycling process, waste concrete is demolished and crushed. The crushed concrete is then sieved and classified as large components (40–200 mm diameter, mainly coarse aggregates), small components (5–40 mm diameter, mainly fine aggregates), and fine powders (<5 mm diameter). The larger components can be reused as aggregates[28, 29]. The fine powders, which are mainly composed of hydrate cement powder, have no effective use. Therefore, the fixation of CO_2 using waste cement powder is advantageous both for the effective use of waste concrete and because waste cement powder is an inexpensive calcium source.

Nitric acid was selected as the acid to leach calcium ions from the waste cement powder because of the very high solubility of calcium nitrate.

In this study, we examined the feasibility of the proposed process based on the experimental studies on the extraction of waste cement powder with nitric acid, which corresponds to step (i), precipitation of calcium carbonate, step (iii), and the regeneration of acid–base pairs by the BMED, step (iv). Since the absorption of CO_2 with alkaline solutions is a well-known process[30, 31], we assume that the alkaline carbonate solution can be generated in an absorption tower with optimum conditions for the other steps.

Materials and Experimental Methods

Characterization of waste cement powder
The waste cement powder used in this study was kindly supplied by Tateishi Construction Co., Ltd. (Tokyo, Japan). The sample was taken from a recycling plant of aggregates from waste concrete. The scanning electron microscope (SEM) image of the sample was taken using a JEOL DATUM JSM-5200 scanning electron microscope (CuKα, 40 kV, 40 mA, JEOL, Tokyo, Japan). The particle size distribution of the waste cement powder was measured with laser-light scattering particle size measurement equipment (SALAD-3000, Shimadzu, Kyoto, Japan).
Elemental analysis of the sample was performed by inductively coupled plasma atomic emission spectroscopy (ICP-AES) using a SPECTRO ARCOS spectrometer (SPECTRO Analytical Instruments, Kleve, Germany) after a two-step dissolution treatment. First, the sample was dissolved in a mixture of nitric acid, hydrochloric acid, and hydrofluoric acid with the assistance of microwave treatment (Actac Speedwave 4, Berghof, Eningen, Germany). Then, boric acid was added into the solution and dissolved with the assistance of microwave treatment.

Extraction experiments of waste cement powder with nitric acid
Extraction experiments with waste cement powder were carried out using nitric acid solution (Reagent grade, Wako Chemicals, Osaka, Japan) of different concentrations ranging from 0.15 to 3.0 M. The waste cement powder sample was sieved, and particles with diameters less than 212 μm were used for the extraction experiments. Waste cement and nitric acid were placed in a 500-mL beaker and mixed with a stirring rate of 200 rpm under the ambient conditions. The mixture was sampled through a syringe with a membrane filter

(pore diameter 0.025 μm) at given time intervals, and the pH change of the solution was monitored with a pH meter (D-51, HORIBA Co., Kyoto, Japan), and the composition of the liquid phase was measured with ICP-AES (Thermo Flex 900, Thermo Fisher Scientific Inc. USA).

Precipitation of calcium carbonate
A known amount of waste cement powder was mixed with nitric acid solution and stirred for a given time at 200 rpm under ambient conditions. The mixture was then filtered with a nitrocellulose filter with a pore diameter of 8.0 μm. The filtered solution was mixed with sodium carbonate solution, and stirred for a given time. The content was filtered with a nitrocellulose filter with a pore diameter of 0.025 μm. The composition of the filtered solution was determined with ICP-AES (Thermo Flex 900, Thermo Fisher Scientific Inc. USA). The precipitant was dried overnight in an oven at 373 K. The solid sample was analyzed using thermogravimetric analysis to determine the calcium carbonate content (SHIMADZU DTG-60H thermal analyzer, Shimadzu, Kyoto, Japan). The content of calcium carbonate was determined by the weight decrease of the sample during the temperature change from 600 to 800°C.

Acid-alkali recovery with bipolar membrane electrodialysis (BMED)
The sodium nitrate solution was subjected to electrodialysis with bipolar membranes (BPED) for the recovery of sodium hydroxide and nitric acid. A schematic drawing of the electrodialysis apparatus is shown in Figure 4. The electrodialysis apparatus is composed of 10 units sandwiched between two electrode cells. The unit is composed of two bipolar membranes (Neosepta BP-1B, ASTOM Co., Japan), and a cation exchange membrane (Selemion CMV, Asahi Glass Co., Japan). The effective membrane area was 0.021 m^2, and the gap between membranes was set at 0.75 mm. The membranes form the acid recovery cells and alkali recovery cells. The feed salt solutions were pumped into the cells with magnetic pumps (Master Flex L/S economy variable speed drive, Cole Parmer) from the feed tanks (0.5 L) at a flow rate of 0.5 L/min, and circulated. Thus, the system is a semi-batch type system. The power was supplied by a direct-current power supply unit (PK36-11, Matsusada Co., Japan).
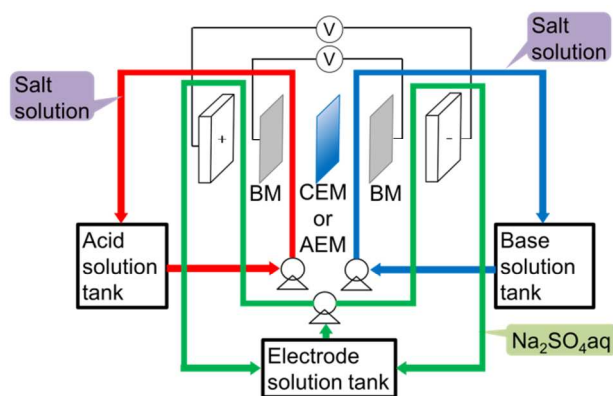
Fig. 4 Schematic drawing for the electrodialysis apparatus for recovery of nitric acid and sodium hydroxide from the sodium nitrate solution. BM: bipolar membrane, and CEM: cation exchange membrane.

The voltage between the outermost bipolar membrane and the electrode was measured to determine the membrane potential.

Sodium sulfate solution (0.1 M) was circulated in the electrode solution with a magnetic pump at a flow rate of 0.4 L/min. After confirming that steady state flow had been achieved, the voltage was applied to the system under constant current conditions. The pH of the solutions was monitored and recorded with a pH meter (D-51, HORIBA Co., Kyoto, Japan). The change of the voltage was measured with a voltmeter (Data Mini, HIOKI Co., Tokyo, Japan). The solution was sampled and the concentrations of nitric acid and sodium hydroxide were determined by the reutilization titration method. The measurement was performed for 120 min, and repeated at least three times to confirm reproducibility.

Results and Discussion

Characterization of waste cement powder

The SEM image of the waste cement powder is shown in Figure 5. The particle size is distributed in the range of 20 μm to several hundred μm, and the surface area-based mean diameter is about 30 μm. The result of elemental analysis is shown in Table 1. The calcium content is the highest at about 32%, followed by the major impurities silicon, aluminum, and iron.
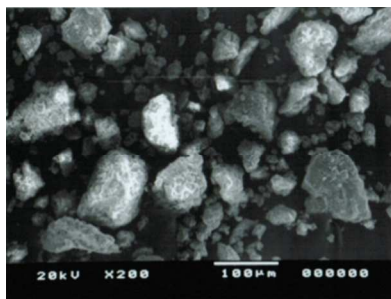

Fig. 5 SEM image of the waste cement powder.

Table 1 Elemental content of the waste cement sample.

Element	Ca	Si	Al	Fe	Mg	Na	K	S
Mass fraction [wt%]	32.25	11.53	2.88	1.75	0.53	0.37	0.29	0.26

Extraction of calcium from waste cement powder

Effect of nitric acid concentration

Figure 6 shows the change of the extraction yield of calcium with extraction time for the various initial concentrations of nitric acid. The extraction yield of calcium is defined as the molar ratio of calcium in the extraction solution to the initial calcium content in the waste cement powder estimated by the elemental analysis (Table 1). For all the runs, the liquid/solid (L/S) ratio was fixed at 20, and the molar ratio of nitric acid to calcium in the waste cement powder (the N/C ratio, hereafter) was consequently changed in the range of 0.38 to 7.7 depending on the concentration of nitric acid. The N/C ratio is shown in the legends of Fig. 6. The extraction yield of calcium rapidly increased after mixing the contents in 10 min, and then was

almost constant during the experiments after that for 24 h (data not shown in Fig. 6). The extraction yield for a given extraction time increased with increasing initial concentration of nitric acid up to 0.60 M, and the maximum yield was about 45%. However, increasing concentration of nitric acid over 0.60 M did not increase the extraction yield. This indicates that the N/C ratio higher than 1.5 does not increase the extraction yield, and about half of calcium containing part would be non-extractable with nitric acid in the waste cement powder.
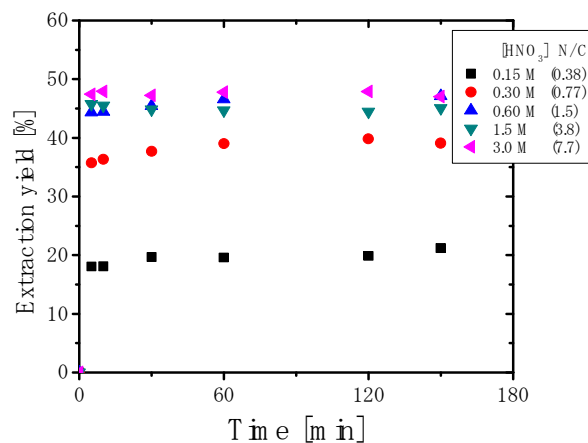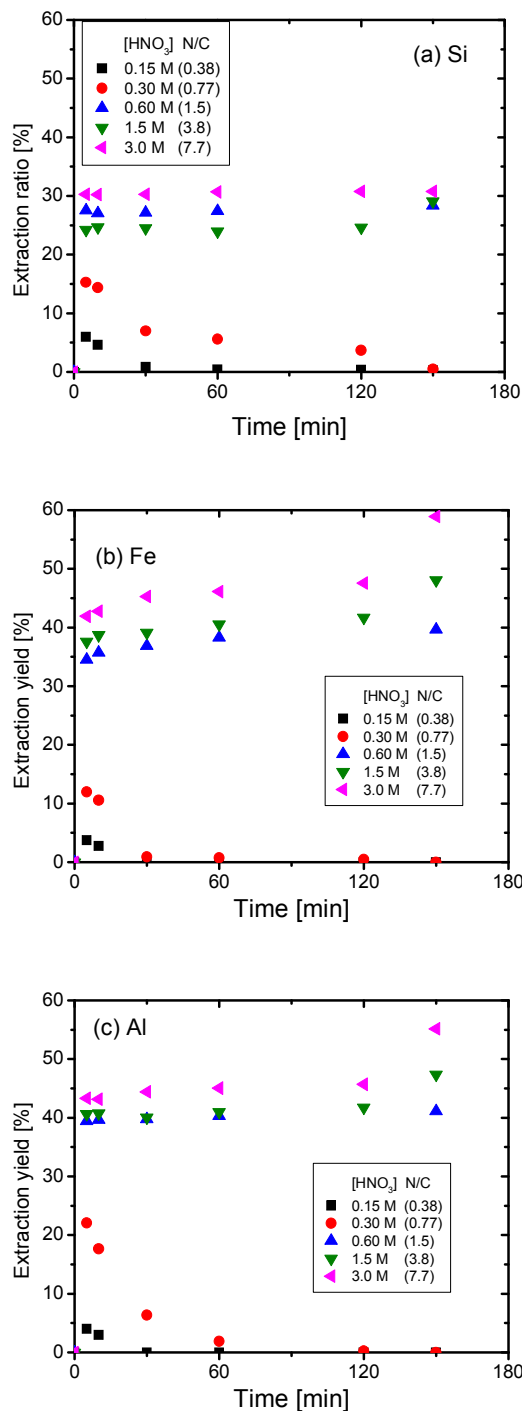

Fig. 6 Change in the calcium extraction yield with extraction time for various initial concentrations of nitric acid (molar ratio of nitric acid and calcium). The L/S ratio was fixed at 20.

Figures 7(a) to 7(c) show the change in the extraction yields of silicon, iron, aluminum, which are major impurities in the waste cement powder, with extraction time for the same conditions in Figure 6. The extraction yield was calculated based on the elemental analysis of waste cement powder (Table 1) and the concentration in the extraction solution. There is a significant gap between the cases with initial concentrations of 0.30 and 0.60 M for the trend of the extraction yield of all the impurities. When the initial concentration of nitric acid was greater than 0.60 M, the extraction yield increased quickly, and increased gradually after that. On the other hand, when the initial concentration of nitric acid was less than 0.30 M, the extraction yield of the impurities first increased with time and then decreased after a certain time. After 150 min, the concentrations of the impurities are almost negligible for the cases with initial nitric acid concentrations of 0.15 or 0.30 M. The weight fraction of calcium in the extraction solution was as high as 99.5% for these cases. On the other hand, the mass fraction of calcium in the extraction solution was about 70% for the cases with the concentration in the range of 0.60 – 3.0 M.

Figure 8 shows the change in pH with extraction time for different initial concentrations of nitric acid. A sharp contrast is observed between the high (≥ 0.6 M) and low (≤ 0.3 M) initial concentrations of nitric acid. When the initial concentration of nitric acid was low, the pH increased with time and almost leveled off at about 9 and 5 for initial nitric acid concentrations of 0.15 and 0.30 M, respectively. On the other hand, the pH remained almost constant at values less than 1 for high nitric acid concentrations (≥ 0.60 M). In strongly acidic conditions (pH < 1), the impurities would be dissolved into the extraction solution, whereas these soluble components would be deposited in the form of hydroxides in high pH conditions. From these results, it is considered that the contamination of impurities in

the extraction solution can be prevented under the conditions reaching higher pH conditions.


Fig. 7 Changes in the extraction yields of impurities (Si, Fe, Al) with extraction time for various initial concentrations of nitric acid. L/S ratio was fixed at 20, same conditions in Fig. 6.
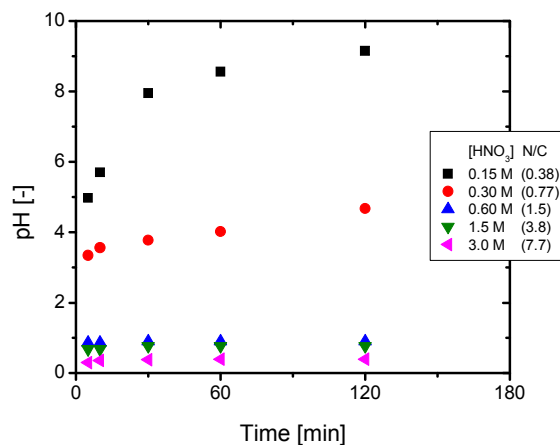
Fig. 8 Change in pH with extraction time for various initial concentrations of nitric acid. The L/S ratio was fixed at 20, same conditions in Fig. 6.

Effect of the solid/liquid ratio

The effect of the weight ratio of nitric acid (L) and the waste cement powder (S), namely, L/S ratio, was examined. The initial concentration nitric acid was fixed at 0.3 M. The L/S ratio was varied in the range 12.5 to 100. The N/C ratio was consequently changed in the range of 0.46 to 3.69. All other experimental conditions were the same as the previous experiments.
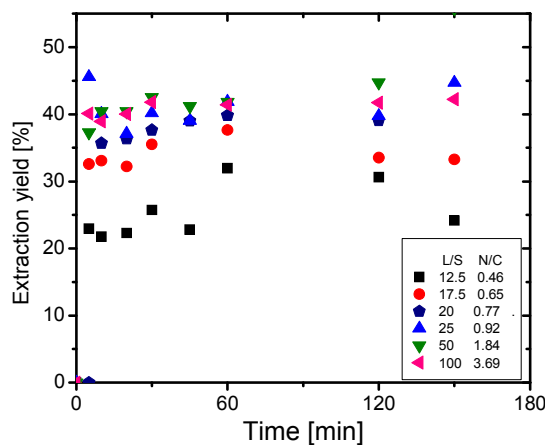
Fig. 9 Change in extraction yield of calcium with time for the various L/S ratios. The initial concentration of nitric acid was fixed at 0.30 M.

Figure 9 shows the change in the extraction yield of calcium for the different L/S ratios with respect to time. The lower L/S (nitric acid to calcium) ratios (12.5 and 17.5) gave the lower extraction yields for a given extraction time, and the extraction yield of calcium was almost unaffected by the L/S ratio higher than 20. Some fluctuations of the extraction yield are observed, which may indicate recrystallization of the extracted calcium. The extraction behavior of the impurities depends on the L/S ratio. When the L/S ratio was high ($\geq$ 25), the extraction yields of the impurities in the extraction solution rapidly

increased after mixing and were almost unchanged thereafter. On the other hand, when the L/S ratio was low (≤ 20), the extraction yields of the impurities initially increased, and then decreased to a negligible level at the later stage. The extraction behaviors of the impurities can be correlated with the pH changes. The pH increased to about 7 to 8 for the lower L/S ratios (≤ 20), while the pH was less than 3 for the higher L/S ratios (≥ 25). The mass fraction of calcium in the extraction solution after 150 min was higher than 99% for the lower L/S ratios (≤ 20), while much lower for the higher L/S ratios. These results suggest that high calcium selectivity can be achieved under the condition of lower L/S ratios, or equivalently, the conditions of lower N/C ratios, that resulted in the higher pH conditions after extraction.

Effect of nitric acid concentration and S/L ratio with a fixed Ca/HNO₃ ratio

The above results demonstrate that higher mass fraction of calcium in the extraction solution can be obtained when the final pH is higher. Such a condition can be achieved when the ratio of nitric acid to calcium in the waste cement (N/C ratio) is lower. In other words, excess calcium conditions are necessary to obtain calcium solution with higher purity in the extraction step.

 In this section, we examined the effect of the initial concentration of nitric acid on the extraction behaviors with a fixed ratio of nitric acid to calcium at N/C = 0.65, which is excess calcium condition relative to nitric acid. The concentration of nitric acid was changed in the range of 0.30 to 3.0 M. Figure 10 shows the changes of the extraction yield of calcium, and mass fraction of calcium in the extraction solution. The calcium extraction yield increased rapidly with time, and almost unchanged after 10 min for all the cases at about 30% for all the cases with different initial concentrations of nitric acid. The mass fraction of calcium in the extraction solution increased with time, and the increasing rate was higher for the cases with higher concentrations of nitric acid. After 120 min, the mass fraction of calcium in the extraction solution reached about 99% for all the cases. The pH change was more rapid for the cases with higher initial concentration of nitric acid. After 120 min, however, all the extraction solutions showed pH higher than 6.5. The observed increase in pH of the extracted solution can be well correlated with the increase in the mass fraction of calcium in the solution.

In summary, the L/S ratio, or equivalently, the N/C ratio is a key factor to determine the calcium extraction yield and the behavior of impurities and pH of the extraction solution. The higher N/C ratio resulted in the higher extraction yield of calcium, but the purity of calcium in the extraction solution was law due to the dissolution of impurities, and the final pH was also low in acidic region. The lower L/S ratio or N/C ratio would give lower extraction yield of calcium, but the extraction rate of calcium was rather high, and the purity of calcium and pH of the extraction solutions are higher. The higher purity of calcium in the extraction solution is favourable for both steps of the precipitation and the BMED. For the precipitation step, the higher purity of calcium in the extraction solution would generate calcium carbonate with higher purity, which may increase the sales values of the product contributing to the cost reduction of the CO₂ fixation process. Foe the BMED step, the higher purity of

the extraction solution is advantageous because the coexisting ions of impurities in the feed salt solution would reduce the current efficiency for the acid-alkali recovery. The higher pH near neutral is critical for the precipitation step because under acidic conditions (pH $<$ pK_{a1} = 6.35), gaseous CO_2 will be released upon mixed with sodium carbonate solution. Under the calcium excess conditions, the calcium extraction yield for a single step would be low; however, the remained waste cement powder after solid-liquid separation could be reused for the next extraction step with the nitric acid regenerated in the BMED step (step (iv)) to increase the overall extraction yield of calcium in the waste cement powder.
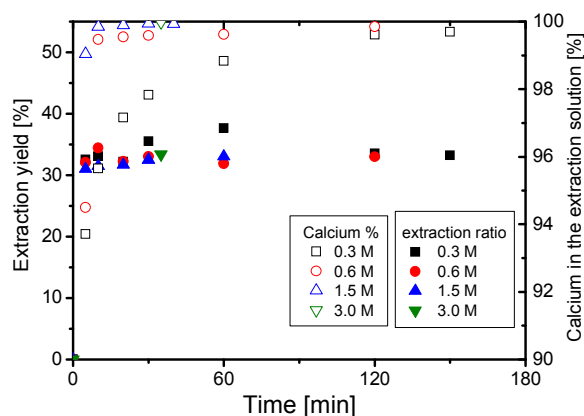

Fig. 10 Time changes in the extraction yield of calcium (left) and the mass fraction of calcium in the extraction solution (right) for the various initial concentrations of nitric acid. The molar ratio of nitric acid to calcium in waste cement (the N/C ratio) was fixed at 0.65.

### Precipitation of calcium carbonate

The extraction solution prepared under the following conditions was used for the precipitation experiment. The extraction condition was as follows. Waste cement powder (57.6 g) was mixed with nitric acid solution (100 mL) of a given molar concentration and stirred for 40 min. The molar ratio of nitric acid to calcium in waste cement powder was N/C = 0.65, a calcium excess condition. The mixture was filtered, and pH of the filtered solution was 7.2. The solution was mixed with sodium carbonate solution (100 mL), of which the molar concentration was half of the nitric acid, and stirred for 30 min. Precipitation occurred immediately upon mixing, and no generation of gaseous CO₂ was observed for all the conditions. The SEM image of the precipitant is shown in Figure 11 for the condition of the initial concentration of nitric acid at 3.0 M, where the diameter of the precipitant was about 10 μm. Figure 12 shows the XRD pattern of the precipitant, indicating that the precipitant is a mixture of calcite and aragonite. The DTA analysis showed that composition of calcium carbonate in the precipitant was higher than 94%. The high purity and small diameter of the obtained calcium carbonate is advantageous for selling as a raw material for the cement production industry or other manufacturing processes.

 The composition of the filtered solution is shown in Table 2 for the condition with the initial concentration of nitric acid at 3.0 M. The calcium concentration decreased from 5.27×10^4 ppm to 378 ppm, indicating that the yield is higher than 99.4%. The remaining

calcium concentration after crystallization was much higher than the concentration estimated from the solubility product of calcium carbonate under atmospheric conditions. This high concentration may be due to remaining calcium nitrate. The calcium concentration is about 1/500 of the sodium concentration (1.5 M), and the influence of the remaining calcium ions in solution on the BMED step for acid and alkaline recovery is negligible. The concentrations of the other impurities contained in the waste cement powder in the solution after crystallization are negligible. Thus, under appropriate extraction conditions, a high-purity solution of sodium nitrate as well as the high-purity calcium carbonate can be obtained in the precipitation step.
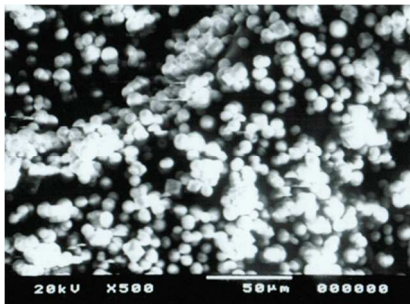
Fig. 11 SEM image of the crystals obtained with precipitation.
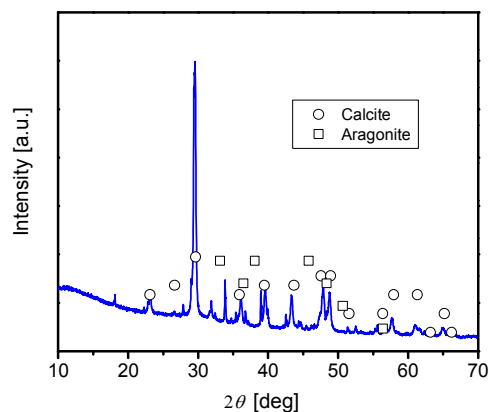
**Fig. 12** XRD spectra of the crystals obtained with precipitation.

Table 2 Elemental composition of the solution before and after the precipitation. Initial concentration of nitric acid = 3.0 M.

Element	Before [ppm]	After [ppm]
Calcium	5.27×10^4	378
Silicon	9.02	1.86
Iron	1.50	< 1.0
Aluminum	2.73	< 1.0

Regeneration of acid and alkali by bipolar membrane electrodialysis

Effect of the current density

Figure 13 shows the changes of the nitric acid concentration and pH in the acid recovery cell and the pH in the alkali recovery cell. The density was set at 0.5 A (current density = 2.4 mA cm^{-2}), and the initial concentration of sodium nitrate in the feed flow was 1.0 M, corresponding to the concentration of nitric acid for the extraction (step (i)) at 1.0 M. The concentration of nitric acid regenerated in BMED almost linearly increased with time up to 30 min, and levelled off after 60 min at about 0.045 M, which corresponds to 4.5% recovery ratio of the initial amount of nitrate ions of 1.0 M. Thus, a very small portion of sodium nitrate in the feed solution can be converted to nitric acid and sodium hydroxide. The pH in the acid recovery cell decreased while that in the alkali recovery cell increased with increasing time. The acid and base can be recovered, but the maximum recovery ratio is low.
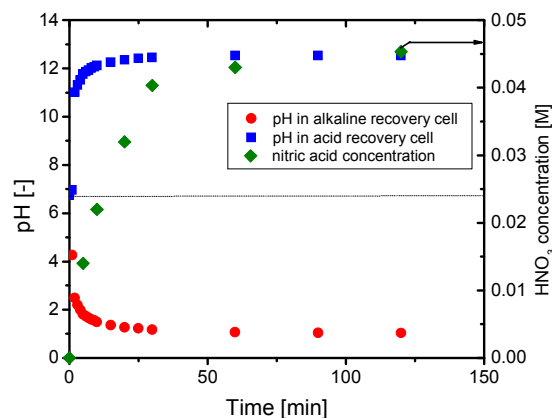
Fig. 13 Time change in pH of the acid and alkali recovery cells (left axis), and nitric acid concentration (right axis) during BMED. Initial concentration of sodium nitrate in the feed = 1.0 M. Current = 0.5 A.

With increasing current, the recovery ratio rapidly increased, and resulted in a higher maximum recovery ratio at high current than at low current, as shown in Figure 14. When the current was 6.0 A, the maximum recovery ratio was 0.44.
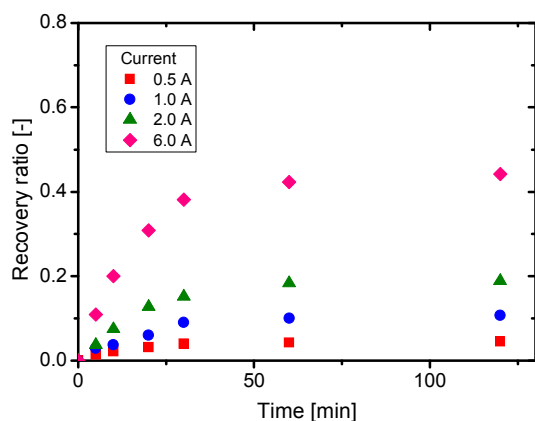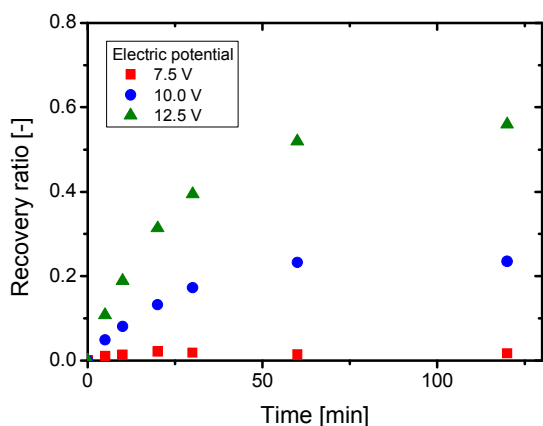
Fig. 14 Time change of the recovery ratio of nitric acid during the BMED under various current conditions. Initial concentration of sodium nitrate in feed = 1.0 M.

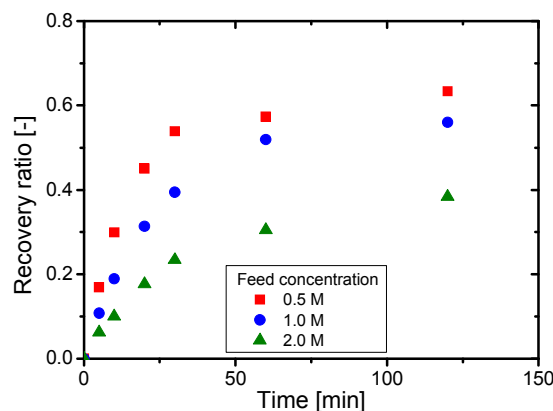### Effect of electric potential

Figure 15 shows the change of the recovery ratio of nitric acid in the acid recovery cell with time for various electric potentials with constant electric potential. The initial feed concentration was 1.0 M. The highest electric potential (12.5 V) resulted in the most rapid increase in the recovery ratio and the highest maximum recovery ratio. The maximum recovery ratio was 0.556 for the electric potential of 12.5 V after 120 min.

Effect of the initial feed concentration

Figure 16 shows the change of the recovery ratio of nitric acid in the acid recovery cell with time for various initial feed concentrations. The highest initial feed concentration (2.0 M) resulted in the slowest increase of the recovery ratio of nitric acid, and a maximum recovery ratio of 0.633 was observed for the initial feed concentration of 0.5 M after 120 min. However, the highest nitric acid and sodium hydroxide concentrations were obtained for the highest initial feed concentration (2.0 M).

Fig. 16 Time changes of the recovery ratio of nitric acid for various initial concentration of feed salt (sodium nitrate) in the feed on the recovery ratio of nitric acid under constant electric potential at 12.5 V.

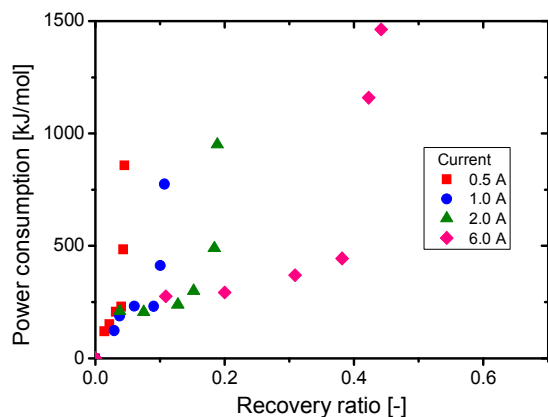### Estimation of the power consumption for the recovery of acid and alkali

Based on the results of the acid and alkali recovery experiments with BMED, the power consumption was estimated. The power consumption, $(P(t))$, for BMED is given by

$$P(t) = I(t)V(t) \tag{7}$$

where $I(t)$ is the current and $V(t)$ is the electric potential between membrane layers. Because both $I(t)$ and $V(t)$ varied with time, power consumption at time t was calculated with a step-by-step method by the power consumption divided by the nitric acid recovered for a given time interval (Eq. (8)).

$$P(t) = \frac{\Delta(IV)}{\Delta n_{HNO3}} = \frac{\{I(t+\Delta t)V(t+\Delta t) - I(t)V(t)\}}{n_{HNO3}(t+\Delta t) - n_{HNO3}(t)} \tag{8}$$

In Figure 17 the power consumption was plotted against the recovery ratio converted from the time for the cases with various currents. The power consumption gradually increased with increasing recovery ratio, owing to the increasing electric resistance in the feed cell where the electrolyte concentration decreased with the transport of ions, and abruptly increased at a certain recovery ratio for each current. The recovery ratio at the abrupt increase was higher for higher currents. Before reaching the recovery ratio at the abrupt increase, the power consumption was almost independent of the current. A similar trend was observed for the effects of electric potential and initial feed concentration. A high electric potential and low initial feed concentration resulted in the highest recovery ratio before the abrupt increase in the power consumption.

Fig. 15 Time changes of recovery ratio of nitric acid for various electric potentials. Initial concentration of sodium nitrate = 1.0 M.

Fig. 17 Change of power consumption against recovery ratio of nitric acid for various currents under a fixed initial concentration of sodium nitrate in the feed at 1.0 M.
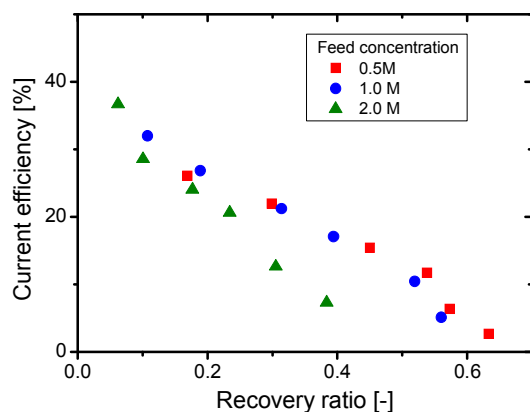
Fig. 18 Change of the current efficiency for the recovery of nitric acid for various feed concentrations, at constant electric potential at 12.5 V.

In Figure 18, the current efficiency is plotted against the recovery ratio. The current efficiency is defined as the ratio of the number of the target ion to be transported to the number of charges transported during electrodialysis. With increasing recovery ratio, the current density monotonously decreased from 40% to less than 10%. This result can be explained in terms of competitive transport of ions: sodium ions and protons, and nitrate ions and hydroxide ions. At the early stages of electrodialysis, the amount of protons in the acid cells was low. The concentration of protons increased with time, and the transport of protons through the cation exchange membrane would compete with the transport of sodium ions. The transport of protons would thus decrease the ion transport number of sodium ions.

From the results of BMED with various conditions, high electric potential, and high current density, the low concentration of sodium nitrate would be favourable for the decrease of power consumption and the recovery of nitric acid and sodium hydroxide.

Summary of the experimental studies and discussion on the operation conditions of the process

The extraction experimental results indicate that the extraction under the lower L/C ratio, or equivalently, lower N/C ratio is favourable for both subsequent steps of the precipitation and the BMED. The BMED experimental results, on the other hand, demonstrated that lower concentrations of the feed salt would be favorable because higher recovery ratio of nitric acid and sodium hydroxide can be achieved with lower power consumption for the lower initial concentrations of the feed salt. The lower salt concentration in the feed fro BMED corresponds to the lower initial concentration of nitric acid in the extraction step. The extraction experimental results showed that the calcium extraction yields and the extraction rate are almost independent of the initial concentration of nitric acid under a fixed N/C ratio. The increasing rate of calcium purity and pH of the extraction solution would be slower for the lower concentrations of nitric acid, but both the final purity and pH are almost independent of the initial concentration of nitric acid. Thus, it is favourable for the extraction step to be performed under the conditions with lower nitric acid and lower N/C ratio, *i.e.*, excess calcium conditions.

In addition, higher electric potential, higher current are also favourable for both in terms of the recovery rate and the power consumption for BMED.

Sulfur dioxide, generated in the power plant, would be absorbed in alkali solution in step (ii) to form sulfate or sulfite ions. These ions can be removed from the system in the precipitation step as precipitants because of low solubility of calcium sulfate and calcium sulfite.

Evaluation of power consumption for CO_2 fixation

Since steps (i) to (iii) are spontaneous processes without consuming power, the total power consumption can be mostly attributable to the power consumption for the BMED process. The power would be also consumed for pumping solutions, solid-liquid separation by filtration or thickener, transportation of waste cement powder and products. Contributions of the additional power consumption are, however, excluded in this study because a rough evaluation of the process is purposed.

In the total process, one mole of CO_2 can be fixed with two moles of sodium hydroxide (equivalent to two moles of nitric acid), and the power consumption for fixation of CO_2 is twice of the power consumption for BMED for acid/alkali recovery shown in Figs. 16-18. The mean specific CO_2 emission is 400 g/kWh (11.8 mol/kWh) for Tokyo Electric Power Company (TEPCO),[32] which is equivalent to power generation at 396 kJ/mol-CO_2 emission. The power consumption for the BMED is normalized by this value to obtain the ratio of power generation in the power plant to the power consumption in the CO_2 fixation. Based on the experimental results, the ratio is below 1 the very early stage of the BMED operation. The present process may not be competitive with other CCS options at the present form. However, the theoretical power consumption for the BMED is determined to be 80.1 kJ for recovery of one mole pair of alkali and acid based on the dissociation energy of water in the bipolar membrane. The theoretical ratio of the power consumption to the power generation per mole CO_2 is thus about 0.2 (80.1 / 396). Therefore, there must be a large room for the improvement of the BMED efficiency.

The measure for improving BMED efficiency would include; increasing the number of cells, increasing the current efficiency by

using more selective ion-exchange membranes, searching the combination of acid and alkali with higher recovery rates, and changing the configuration of electrodialysis, such as using anion exchange membranes instead of cation exchange membranes. In future studies, we will study the effect of these parameters on the electrodialysis efficiency.

The cost for the regeneration of acid and alkaline can be estimated by the price of electric power at 0.07 USD per kWh. Suppose the recovery ratio is 0.2 in Figure 19 for the initial concentration at 0.5 M. The power consumption is 300 kJ/mol, and 600 kJ/mol-CO_2. For 1 metric ton of CO_2, the power consumption is 3800 kWh, which is about 260 USD (about €200). The cost is relatively high compared to the cost reported for other mineral carbonation methods in the range of €25 to €258. [33] The cost for the present process is, at the present stage, is higher than the previous processes. There are, however, some merits of the present process. First, the electrodialysis process requires direct-current power, and the scale merit of the system is insignificant. Thus, it is more appropriate to use renewable energy sources such as photovoltaic cells, wind power, and tidal power. The use of renewable energy sources could be applied to stand-alone CO_2 fixation systems. In addition, the present process can be recognized as a waste treatment process for a building waste, waste cement powder, which has no effective use. When the product, calcium carbonate, is used for production of cement, the CO_2 emission from virgin lime stone could be reduced. The reduction of the CO_2 emission by the present process can be considered as a carbon offset measure.

Conclusions

The feasibility of the process of CO_2 fixation with waste cement powder electrodialysis was examined. High-purity calcium carbonate (> 97%) was obtained under appropriate conditions where the final pH of the solution was about 7. Electrodialysis was performed on the remaining solution of sodium nitrate, and nitric acid and sodium hydroxide was recovered with relatively high purity. High current density, high voltage, and low concentration of the feed solution of sodium nitrate are favourable in terms of power consumption. Improvement for the efficiency of the process would make the present process as an option of a mineral carbonation process for CCS.

Notes and references

[a] *Graduate School of Science and Engineering, Seikei University, 3-3-1 Kichijoji-kitamachi, Musashino, Tokyo 180-8633, Japan*

[b] *Department of Chemical Engineering, Hiroshima University, Higashi-Hiroshima, Hiroshima 739-8527, Japan*

[c] *Research Center for Sustainable Science and Engineering, Institute of Multidisciplinary Research for Advanced Materials, Tohoku University, 2-1-1 Katahira, Sendai, Miyagi 980-8577, Japan*

1 B. Metz, O. Davidson, H. de Coninck, M. Loos, L. Meyer, *IPCC special report on carbon dioxide capture and storage*, Intergovernmental Panel on Climate Change (IPCC), Working Group III, Geneva, 2005.

2 M. E. Boot-Handford, J. C. Abanades, E. J. Anthony, M. J. Blunt, S. Brandani, N. MacDowell, J. R. Fernández, M.–C. Ferrari, R. Gross, J. P. Hallett, R. S. Haszeldine, P. Heptonstall, A. Lyngfelt, Z. Makuch, E. Mangano, R. T. J. Porter, M. Pourkashanian, G. T. Rochelle, N. Shah, J. G. Yao, P. S. Fennell, *Energy Environ. Sci.*, 2014, **7**, 130.

3 N. MacDowell, N. Florin, A. Buchard, J. Hallett, A. Galindo, G. Jackson, C. S. Adjiman, C. K. Williams, N. Shah, P. Fennell, *Energy Environ. Sci.*, 2010, **3**, 1645.

4 R. Zevenhoven, J. Fagerlund, J. K. Songok, *Greenhouse Gas Sci. Technol.*, 2011, **1**, 48.

5 S.-Y. Pan, E.E. Chang, P.-C. Chiang, *Aerosol Air Quality Research*, 2012, **12**, 770.

6 A. A.Olajire, *J. Petroleum Sci. Eng.*, 2013, **109**, 364.

7 M. Kakizawa, A. Yamasaki, Y. Yanagisawa, *Energy*, 2004, **26**, 341.

8 Z. Y. Chen, W. K. O'Connor, S. J. Gerdemann, *Environ. Prog.*, 2006, **25**, 161.

9 S. Teir, H. Revitzer, S. Eloneva, C. J. Fogelholm, R. Zevenhoven, *Int. J. Miner. Process.*, 2007, **86**, 36.

10 A. Iizuka, M. Fujii, A. Yamasaki, Y. Yanagisawa, *Ind. Eng. Chem. Res.*, 2004, **43**, 7880.

11 S. Eloneva, S. Teir, H. Revitzer, J. Salminen, A. Said, C. J. Fogelholm, R. Zevenhoven, *Steel Res. Int.*, 2009, **80**, 415.

12 S. Eloneva, S. Teir, J. Salminen, C. J. Fogelholm, R. Zevenhoven, *Energy.*, 2008, **33**, 1461.

13 G. Jones, G. Joshi, M. Clark, D. McConchie, *Environ. Chem.*, 2006, **3**, 297.

14 Z. Y. Chen, W. K. O'Connor, *Green Chem.*, 2004, **6**, 428.

15 A. Iizuka, Y. Sakai, A. Yamasaki, M. Honma, Y. Hayakawa, Y. Yanagisawa, *Ind. Eng. Chem. Res.*, 2012, **51**, 6099.

16 G. Alexander, M. M. Maroto-Valer, P. Gafarova-Aksoy, *Fuel*, 2007, **86**, 273.

17 S. Teir, S., R. Kuusik, C. J. Fogelholm, R. Zevenhoven, *Int. J. Miner. Process.*, 2007, **85**, 1.

18 S. Teir, S. Eloneva, C. J. Fogelholm, R. Zevenhoven, *Appl. Energy*, 2009, **86**, 214.

19 A. Iizuka, Ph.D. Thesis, University of Tokyo, 2006.

20 W. K. O'Connor, D. C. Dahlin, D. N. Nilsen, R. P. Walters, P. C. Turner, *Proceedings of the 25th International Technical Conference on Coal Utilization & Fuel Systems*, Coal Technology Association, Clearwater, Florida, 2000.

21 S. Teir, S. Eloneva, C. J. Fogelholm, R. Zevenhoven, *Energy*, 2007, **32**, 528.

22 A. J. B. Kemperman, *Handbook on bipolar membrane technology*, Twente University Press, Enschede, The Netherlands, 2000, pp. 241-275.

23 C. Huang, T. Xu, *Environ. Sci. Technol.*, 2006, **40**, 5233-5243.

24 Ministry of Land, Infrastructure, Transport and Tourism, Japan, On the results of construction waste emission survey in 2006, http://www.mlit.go.jp/report/press/sogo20_hh_000012.html, accessed November, 2013.

25 Waste treatment and IPPC DG ENV Workshop, Brussels, 26 January 2007, Background paper, http://circa.europa.eu/Public/irc/env/ippc_rev/library?l=/gathering_activities/workshop_treatment/background_ippcwastepdf/_EN_1.0_&a=d, accessed November, 2013.

26 United States Environmental Protection Agency, Estimating 2003 Building-Related Construction and Demolition Materials Amounts, http://www.epa.gov/wastes/conserve/imr/cdm/pubs/cd-meas.pdf, accessed November, 2013.

27 J. Shi, Y. Xu, *Resour. Conserv. Recy.*, 2006, **49**, 147.

28 A. Rao, K. N. Jha, S. Misra, *Resources, Conservation and Recycling*, 2007, **50**, 71.

29 A. Iizuka, M. Nakagawa, K. Kumagai, A. Yamasaki, Y. Yanagisawa, *J. Chem. Eng. Japan*, 2010, **43**, 906.

30 R. H. Perry and D. W. Green ed., Perry's Chemical Engineers' Handbook, 7th ed., Section 14, McGraw-Hill, New York, 1997.

31 A. Iizuka, K. Hashimoto, H. Nagasawa, K. Kumagai, Y. Yanagisawa, A. Yamasaki, *Separation and Purification Technology*, 2012, **101**, 49.

32 Tokyo Electric Power Company website, Report on the CO_2 emission and specific CO_2 emission in 2010, http://www.tepco.co.jp/cc/press/11110702-j.html, accessed November, 2013.

33 W.J.J. Huijgen, R.N.J. Comans, G.-J. Witkamp, *Energy Convers. Management*, 2007, **48**, 1923.

RSC Advances Accepted Manuscript